

2 Unfolding the relation between global temperature and ENSO

3 A. A. Tsonis,¹ J. B. Elsner,² A. G. Hunt,³ and T. H. Jagger²

4 Received 1 March 2005; revised 25 March 2005; accepted 30 March 2005; published XX Month 2005.

6 [1] An analysis of global temperature and ENSO data
7 indicates that their relationship is more complicated than
8 currently thought. Indeed, it appears that there are two
9 complimenting aspects to this relation. The first (and
10 known) aspect expresses the fact that global temperature
11 increases after an El Nino event and a La Nina event follows
12 an El Nino event. Thus, El Nino forces global temperature.
13 While this is an important result, it is not the entire picture.
14 If it were, ENSO would be independent of global
15 temperature. The second aspect, which is proposed here,
16 suggests a deeper connection between global temperature
17 and ENSO. We find that ENSO is not independent and that
18 positive (negative) global temperature tendency tends to
19 trigger an El Nino (La Nina). Thus, in a warming climate
20 El Nino events will be more frequent than La Nina events.
21 The methodology presented in this paper may elucidate
22 how realistically coupled ocean-atmosphere models
23 simulate the response of climate to global change.
24 **Citation:** Tsonis, A. A., J. B. Elsner, A. G. Hunt, and T. H.
25 Jagger (2005), Unfolding the relation between global temperature
26 and ENSO, *Geophys. Res. Lett.*, 32, LXXXXX, doi:10.1029/
27 2005GL022875.

29 1. Introduction

30 [2] Under normal conditions the westward equatorial
31 trade winds of the tropical Pacific force equatorial Rossby
32 waves, which pile up warm surface water toward the west.
33 This deepens the equatorial thermocline in the west creating
34 a thermal reservoir and raises it in the east causing upwell-
35 ing of cold water to the surface in the east. Warming in the
36 west and cooling in the east is enhanced during a La Nina
37 event. A weakening or reversal of the trade winds (through
38 anomalous westerly wind bursts) initiates Kelvin waves,
39 which travel eastward and which reduce the upwelling
40 thereby diminishing the thermal contrast between west
41 and east. At the same time the warm surface water above
42 the thermocline sloshes back and spreads to the east
43 producing a large area of warm surface water in the eastern
44 Pacific Ocean called an El Nino event. During both events
45 increased convection over the warm surface provides a
46 positive feedback mechanism that leads to either enhanced
47 trade winds (during La Nina) or anomalous westerly winds
48 (during El Nino). While the build up of heat content in the
49 west may set the stage for the development of an El Nino,
50 ENSO is often modulated by higher frequency variability.

This variability may arise from the Madden-Julian Oscilla- 51
tion (MJO) [*Madden and Julian, 1972*], which produces 52
westerly wind events, which in turn can generate Kelvin 53
waves as they propagate eastward [*McPhaden, 1999*]. 54
Kelvin waves can also be generated by Rossby waves 55
reflecting at the western boundary. These Kelvin waves 56
take a few months to traverse the Pacific introducing a time 57
lag between the trigger and surface warming in the east. The 58
net result is a complex aperiodic phenomenon. 59

[3] The processes described above comprise modern 60
theories and models of ENSO evolution [*Battisti, 1988*; 61
Schopf and Suarez, 1987; *Suarez and Schopf, 1988*; *Zebiak* 62
and Cane, 1987; *Neelin et al., 1998*; *Blanke et al., 1997*; 63
Fedorov, 2002; *Penland and Matrosova, 1994*]. These 64
theories and models, however, have yet to explain the fine 65
details behind the initiation of an event and the role global 66
change plays. For example, what is the origin of the 67
anomalous wind bursts? Why in the period 1976–1998 68
has there been several strong El Nino events and hardly 69
any La Nina events? Why do the models not respond the 70
same way as global temperature changes [*Timmermann et* 71
al., 1999; *Collins, 2000*; *Collins et al., 2005*]? This 72
paper examines the relationship of global temperature 73
and ENSO and offers some answers to the above 74
questions. 75

2. Data Analysis and Results 76

[4] We begin by considering the cross-correlation 77
between global temperature, T , and the Southern Oscillation 78
Index (SOI) where the temperatures are from the detrended 79
Intergovernmental Panel for Climate Change (IPCC) record. 80
In order to make direct connections between higher (lower) 81
temperatures and El Nino (La Nina) frequency of occur- 82
rence we reverse the SOI sign so that positive values 83
indicate El Nino and negative values indicate La Nina. 84
We observe (Figure 1a) that the cross-correlation structure is 85
characterized on the average by positive correlations for 86
positive lags (when SOI leads T). This indicates that El 87
Ninos precede higher global temperatures and La Ninas 88
precede lower global temperatures. At the same time we 89
observe a general tendency for negative correlations for 90
negative lags (when T leads SOI). This indicates that lower 91
global temperatures precede El Nino events and higher 92
global temperatures precede La Nina events. Similar results 93
are obtained when instead of SOI we use the N3.4 index 94
(Figure 1b). Thus, Figure 1 displays the well-known result 95
that El Nino tends to increase the average temperature of the 96
planet and that in general a La Nina succeeds an El Nino. 97
Mechanisms for this warmth can be traced to changes in 98
cloudiness and atmospheric circulations [*Trenberth et al.,* 99
2002; *Klein et al., 1999*; *Kumar and Hoerling, 2003*]. Next, 100
we present results that add another piece to the puzzle of the 101
relationship between ENSO and global temperature. 102

¹Atmospheric Sciences Group, Department of Mathematical Sciences,
University of Wisconsin-Milwaukee, Milwaukee, Wisconsin, USA.

²Department of Geography, Florida State University, Tallahassee,
Florida, USA.

³Department of Physics, Wright State University, Dayton, Ohio, USA.

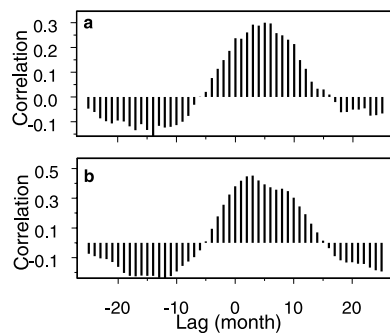


Figure 1. (a) Time domain analysis of global temperature and ENSO. This graph shows the cross-correlation between global temperature and negative values of the SOI based on 1248 consecutive months from 1900–2003. The overall trend in the global temperature is removed. (b) Same as Figure 1a but when the N3.4 index is used instead of SOI. The values of N3.4 are based on data from 1950–2003. N3.4 is the average sea surface temperature in the box 5°N – 5°S , 170°W – 120°W .

[5] Figure 2a shows the cross-correlation between SOI and the $\Delta T/\Delta t$ function (for $\Delta t = 1$ month) for positive lags (SOI leads ΔT) and for negative lags (ΔT leads SOI). Two important points come out of this analysis. First, there is a peak at about lag = -5 months with positive correlations and a peak at about lag = $+11$ months with negative correlations. This overall variation of the cross-correlation indicates a 30–40 month coherency. Superimposed on this cycle is a high frequency oscillation of about three months. Because the correlations are not large, we test the statistical significance of these two oscillations in the cross-correlation function using coherency analysis in the frequency domain. Figure 2b shows the squared coherency between global temperature and SOI. Coherence measures the linear dependence of the oscillatory components in the two detrended signals. While it does not indicate cause and effect, significant coherence suggests that changes in one signal relate to changes in the other signal. When the squared coherency is transformed by the inverse hyperbolic tangent, the resulting values have a normal distribution centered on zero and with a variance proportional to the sum of squares of the smoothing weights [Kuo *et al.*, 1990]. This allows us to make a correspondence between the values of squared coherency and confidence levels. For example, for a given frequency, squared coherency values of 0.2 and 0.25 define the approximate 90% and 95% confidence levels, respectively, for incoherent series. Accordingly, Figure 1b indicates that the coherence between temporal changes in T and SOI is high in the frequency band centered at about 0.32 cycles/month and exceptionally high in the frequency band centered at about 0.028 cycles/month. These statistically significant coherency bands correspond to time scales of three and 36 months observed in the time analysis and are similar to the time scales of Kelvin waves and the El Nino/La Nina cycle, respectively. It thus appears that processes associated with these two major time scales largely determine the cross-correlation structure between changes in global temperature and SOI. This agrees well with the evolution of ENSO discussed above. Phase estimates of the coherence (not shown)

indicate that in the high frequency coherent band, temperature fluctuations lead SOI by about three months. Since this band is in the Kelvin wave scale, this implies that temperature fluctuations may precede Kelvin wave formation. Since Kelvin wave formation is due to a westerly wind stress anomaly, it follows that anomalous westerly wind bursts may be modulated by global temperature changes. This is an important finding as it ties global temperature fluctuations directly to the emergence of the anomalous wind bursts and thus in the triggering of El Nino.

[6] Second, the positive correlations in Figure 2a when ΔT leads SOI indicate that positive (negative) temperature fluctuations precede El Nino (La Nina) development. At the same time, the negative correlations when SOI leads ΔT indicate that El Nino (La Nina) relate to future negative (positive) temperature tendencies. This suggests that a positive (negative) global temperature tendency triggers an El Nino (La Nina), which ultimately reverses the tendency. True enough (as we show in Figure 1) once an El Nino is initiated and warm water spreads over a significant portion of the planet, the global mean temperature will increase (also as mentioned above other mechanisms contribute to this warming). Thus, initially the role of El Nino is to support the positive tendency. Note that the contribution of ENSO to the long-term temperature trend in the last 50 years is about 0.06°C or 10% of the overall trend [Trenberth *et al.*, 2002]. However, as Figure 2a indicates, after a time scale of the order of 16 ($5 + 11$) months, El Nino's role is to reverse that tendency. This is in agreement with others who have observed that it takes 16–18 months for El Nino to deplete the storage of heat in the west part of the Pacific basin [Neelin *et al.*, 1998]. After El Niño has run its course, the stored heat in the equatorial and off-equatorial Pacific is eliminated as it disperses in the atmosphere and is transported poleward by ocean currents to be incorporated in the

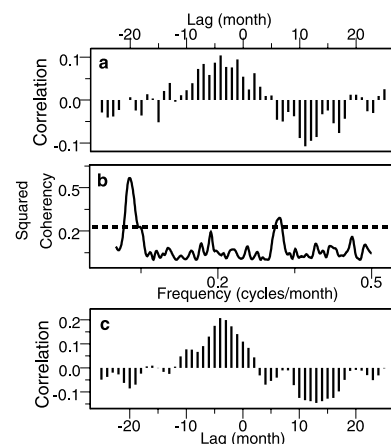


Figure 2. Time and frequency domain analysis of global temperature tendency and ENSO. (a) Cross-correlations of temperature tendency and negative values of the SOI. (b) Square coherency between global temperature and SOI. The broken horizontal line indicates the approximate 90% significance level. The squared coherency is smoothed using a “Daniell” window and a taper of 0.1. (c) Same as Figure 2a but when the N3.4 values are used instead of the SOI values.

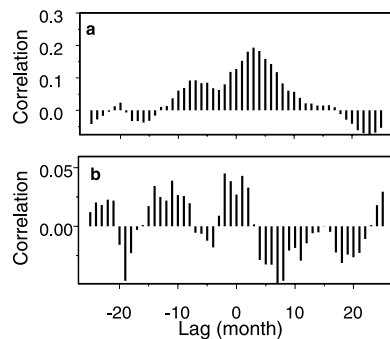


Figure 3. (a) Same as Figure 1b but using global temperature and ENSO data from a 119-year CSM simulation. (b) Same as Figure 2c but using data from a 119-year CSM simulation.

178 formation of mid-latitude storms [Wang *et al.*, 2003; Lau *et al.*, 2004; Sun and Trenberth, 1998]. This leads to a
 179 reduction in atmospheric temperatures as heat is again
 180 deposited in the thermal reservoir in the western Pacific.
 181 Analogous arguments hold for La Nina. This result is in
 182 agreement with previous work investigating scaling prop-
 183 erties of global temperature records that show a change
 184 from persistence (Hurst exponent $> 1/2$) to self-correction
 185 (Hurst exponent $< 1/2$) [Tsonis *et al.*, 1998] at time scales
 186 relevant to ENSO. Similar results hold when the Nino
 187 3.4 (N3.4) index is used instead of the SOI (Figure 2c).
 188 The idea that ENSO acts as a ‘safety valve’ in the climate
 189 system is consistent with the ‘heat pump’ hypothesis for
 190 ENSO, which states that ENSO helps to shed excess heat in
 191 the tropics [Sun and Trenberth, 1998; Sun, 2000].

192 [7] The physics behind the above results is complex but
 193 well understood. An increase in global temperature leads to
 194 a rapid (and greater) heat storage in the tropical Pacific
 195 [Latif *et al.*, 1997]. Increased heat storage leads to stronger
 196 trade winds [Latif *et al.*, 1997; Shriver and O’Brien, 1995].
 197 Scaling arguments for turbulent flow in boundary layers as
 198 well as thermodynamic arguments dictate that an increase in
 199 trade wind strength induces an increase in trade wind
 200 fluctuations [Kolmogorov, 1941]. If this were not true the
 201 system must have negative absolute temperatures. These
 202 wind fluctuations, however, will not trigger El Ninos and La
 203 Ninas with equal chance. With rapid storage of energy the
 204 thermal and physical inertia of the regions of heat storage in
 205 the western Pacific increase more rapidly, with a tendency
 206 for enhanced sea surface elevation gradients. These
 207 gradients suppress the triggering of La Nina, even when
 208 the trade winds are stronger and fluctuations are larger.
 209 Thus, when global temperatures are on the rise, El Nino is
 210 favored over La Nina. A corollary of the above is that in a
 211 scenario of a sustained positive (negative) global tempera-
 212 ture tendency (which will result in a positive (negative)
 213 long-term trend), the frequency of El Nino events will be
 214 greater (less) than that of La Nina events. Recent observa-
 215 tions support this conclusion. In the period 1976–1998 the
 216 globe experienced a pronounced positive temperature trend
 217 and several strong El Nino events but hardly any La Nina
 218 events. The same is true for the period of rising tempera-
 219 tures at the beginning of the 20th century (1900–1925)
 220 when El Nino events were more frequent. In contrast during
 221

the period 1925–1975 when no marked positive or negative
 222 temperature trend was observed, El Nino and La Nina
 223 occurred with similar frequency. Note that the results agree
 224 with the theory on the relation between global change and
 225 ENSO recently proposed by Tsonis *et al.* [2003]. It follows
 226 that this second aspect in the relation between global
 227 temperature and ENSO is backed by physical mechanisms
 228 and it is consistent with the observed frequency of El Nino
 229 and La Nina and with previous work. Note that we are not
 230 claiming that there will be more El Nino events with a
 231 warmer planet (an issue which is still open), but rather more
 232 El Nino events with a *warming* planet.
 233

[8] We thus see that there are two aspects in the relation
 234 between global temperature and ENSO. The first is the well-
 235 known result that El Nino tends to increase the average
 236 temperature of the planet. The second aspect is more
 237 complex as it indicates that global temperature fluctuations
 238 provide the triggering mechanism and that once an event is
 239 triggered it eventually acts to reverse the sign of the
 240 fluctuation. These two aspects form a negative feedback
 241 loop which controls runaway tendencies.
 242

3. A Test for Models

[9] As was mentioned above coupled ocean/atmosphere
 244 GCMs do not universally agree on how they respond to a
 245 warmer global temperature. The method presented here can
 246 be used on model simulations to verify whether or not a
 247 model realistically simulates the ENSO cycle. If a model
 248 simulation reproduces to a good degree the two aspects of
 249 the relation between global temperature and ENSO, then the
 250 model simulates the cycle realistically. As an example we
 251 test NCAR’s Climate System Model 1 (CSM1). We use the
 252 output of a 119-year experiment in which the global
 253 temperature is forced to increase by a rising CO_2 concen-
 254 tration rate of 1%/year from its pre-industrial level (case
 255 b006, data accessible at www.ucar.edu). First we compute
 256 the monthly mean surface global and N3.4 temperature.
 257 Then we remove the annual cycle by computing monthly
 258 anomalies and repeat the above correlation/coherence anal-
 259 ysis. Although the correlations are generally smaller, the
 260 results from this model are qualitatively similar to those
 261 in Figures 1 and 2. Figure 3a is similar to Figure 1b and
 262 Figure 3b to Figure 2c but using the model output. By
 263 comparing 3a and 1b we find that the cross-correlation
 264 functions have the same sign in 39 out of 51 lags. From
 265 Figures 3b and 2c we find that that the cross-correlation
 266 functions have the same sign in 35 out of 51 lags. Thus, this
 267 model simulation agrees with the observed cross-correlation
 268 function between T and N3.4 in 76% of the lags and with
 269 the observed cross-correlation function between ΔT and
 270 N3.4 in 68% of the lags.
 271

[10] Moreover, this model output confirms the corollary
 272 that in a scenario of a sustained positive (negative) global
 273 temperature tendency, the frequency of El Nino events
 274 will be greater (less) than that of La Nina events. In this
 275 120-year simulation, the El Nino frequency is 20/century,
 276 while the La Nina frequency is 11/century. On the contrary,
 277 in a 300-year steady state experiment with the same model
 278 (case b003), El Nino and La Nina events occur at roughly
 279 the same frequency (about 17 events/century). Here an
 280 event is defined as greater than a one standard deviation
 281

282 from the mean N3.4 index, which persists at least 6 months
 283 (positive departures for El Niño). Even though not perfectly,
 284 this model appears to capture qualitatively and quantitatively
 285 both aspects of the observed relation between global tem-
 286 perature and ENSO.

287 4. Conclusions

288 [11] We present evidence that establishes a clearer picture
 289 of how global change relates to ENSO variability. The most
 290 important result is that positive temperature fluctuations
 291 tend to trigger an El Niño and negative fluctuations tend
 292 to trigger a La Niña; a result that provides an observational
 293 target for coupled ocean-atmosphere models. This result is
 294 supported by physical arguments, observations, past work
 295 and model simulations. It follows, that in a warming climate
 296 the frequency of El Niño events will be greater than the
 297 frequency of La Niña events. This makes global temperature
 298 change (which can be either the result of natural variability
 299 and/or the result of anthropogenic effects) an important
 300 input to ENSO dynamics. Since ENSO effects are world-
 301 wide, this makes predictions of global temperature trends of
 302 paramount importance in forecasting changes in weather
 303 patterns in the 21st century.

304 [12] **Acknowledgment.** We thank Kyle Swanson for help with the
 305 CSM data.

306 References

307 Battisti, D. S. (1988), Dynamics and thermodynamics of a warming event
 308 in a coupled tropical atmosphere-ocean model, *J. Atmos. Sci.*, *45*, 2889–
 309 2919.
 310 Blanke, B., J. D. Neelin, and D. Gutzler (1997), Estimating the effect
 311 of stochastic wind forcing on ENSO irregularity, *J. Clim.*, *10*, 1473–
 312 1486.
 313 Collins, M. (2000), The El Niño–Southern Oscillation in the second
 314 Hadley Centre coupled model and its response to greenhouse warming,
 315 *J. Clim.*, *13*, 1299–1312.
 316 Collins, M., and the CMIP Modeling Groups (2005), El Niño- or La Niña-
 317 like climate change?, *Clim. Dyn.*, in press.
 318 Fedorov, A. V. (2002), The response of the coupled tropical ocean-atmosphere
 319 to westerly wind bursts, *Q. J. R. Meteorol. Soc.*, *128*, 1–23.
 320 Kolmogorov, A. N. (1941), Dissipation of energy in locally isotropic
 321 turbulence, *Dokl. Akad. Nauk SSSR*, *32*, 16–18.
 322 Klein, S. A., B. J. Soden, and N.-C. Lau (1999), Remote sea surface
 323 temperature variations during ENSO: Evidence for a tropical atmospheric
 324 bridge, *J. Clim.*, *12*, 917–932.
 325 Kumar, A., and M. P. Hoerling (2003), The nature and causes for
 326 the delayed atmospheric response to El Niño, *J. Clim.*, *16*, 1391–
 327 1403.

Kuo, C., C. Lindeberg, and D. J. Thomson (1990), Coherence established
 328 between atmospheric carbon dioxide and global temperature, *Nature*,
 329 *343*, 709–714. 330
 Latif, M., R. Kleeman, and C. Eckert (1997), Greenhouse warming, decadal
 331 variability or El Niño? An attempt to understand the anomalous 1990's,
 332 *J. Clim.*, *10*, 2221–2239. 333
 Lau, K. M., J. Y. Lee, K. M. Kim, and I. S. Kang (2004), The North Pacific
 334 as a regulator of summertime climate over Eurasia and North America,
 335 *J. Clim.*, *17*, 819–833. 336
 Madden, R. A., and P. R. Julian (1972), Description of global scale circula-
 337 tion cells in the tropics with 40–50 day period, *J. Atmos. Sci.*, *29*, 1109–
 338 1123. 339
 McPhaden, M. J. (1999), Genesis and evolution of the 1997–98 El Niño,
 340 *Science*, *283*, 950–954. 341
 Neelin, J. D., D. S. Battisti, A. C. Hirst, and F.-F. Jin (1998), ENSO
 342 theories, *J. Geophys. Res.*, *103*, 14,261–14,290. 343
 Penland, C., and L. Matrosova (1994), A balance condition for numerical
 344 models with applications to El Niño–Southern Oscillation, *J. Clim.*, *7*,
 345 1352–1372. 346
 Schopf, P. S., and M. J. Suarez (1987), Vacillations in a coupled ocean-
 347 atmosphere model, *J. Atmos. Sci.*, *45*, 549–566. 348
 Shriver, J. F., and J. J. O'Brien (1995), Low frequency variability of the
 349 equatorial Pacific Ocean using a new pseudostress dataset: 1930–1989,
 350 *J. Clim.*, *8*, 2762–2786. 351
 Suarez, M. J., and P. S. Schopf (1988), A delayed action oscillator for
 352 ENSO, *J. Atmos. Sci.*, *45*, 3283–3287. 353
 Sun, D.-Z. (2000), The heat sources and sinks of the 1986–87 El Niño,
 354 *J. Clim.*, *13*, 3533–3550. 355
 Sun, D.-Z., and K. Trenberth (1998), Coordinated heat removal from the
 356 equatorial Pacific during the 1986–87 El Niño, *Geophys. Res. Lett.*, *25*,
 357 2659–2662. 358
 Timmermann, A., et al. (1999), Increased El Niño frequency in a
 359 climate model forced by future greenhouse warming, *Nature*, *398*,
 360 694–696. 361
 Trenberth, K. E., J. M. Caron, D. P. Stepaniak, and S. Worley (2002),
 362 Evolution of El Niño–Southern Oscillation and global atmospheric
 363 surface temperatures, *J. Geophys. Res.*, *107*(D8), 4065, doi:10.1029/
 364 2000JD000298. 365
 Tsonis, A. A., P. J. Roebber, and J. B. Elsner (1998), A characteristic time
 366 scale in the global temperature record, *Geophys. Res. Lett.*, *25*, 2821–
 367 2823. 368
 Tsonis, A. A., A. G. Hunt, and J. B. Elsner (2003), On the relation
 369 between ENSO and global climate change, *Meteorol. Atmos. Phys.*, *84*,
 370 229–242. 371
 Wang, X. C., F. F. Jin, and Y. Q. Wan (2003), A tropical ocean recharge
 372 mechanism for climate variability. Part I: Equatorial heat content changes
 373 induced by the off-equatorial wind, *J. Clim.*, *16*, 3585–3598. 374
 Zebiak, S. E., and M. A. Cane (1987), A model El Niño/Southern Oscilla-
 375 tion, *Mon. Weather Rev.*, *115*, 2262–2278. 376

J. B. Elsner and T. H. Jagger, Department of Geography, Florida State
 378 University, Tallahassee, FL 32306, USA. 379

A. G. Hunt, Department of Physics, Wright State University, Dayton, OH
 380 45435, USA. 381

A. A. Tsonis, Atmospheric Sciences Group, Department of Mathe-
 382 matical Sciences, University of Wisconsin-Milwaukee, Milwaukee, WI
 383 43201-0413, USA. (aatsonis@uwm.edu) 384